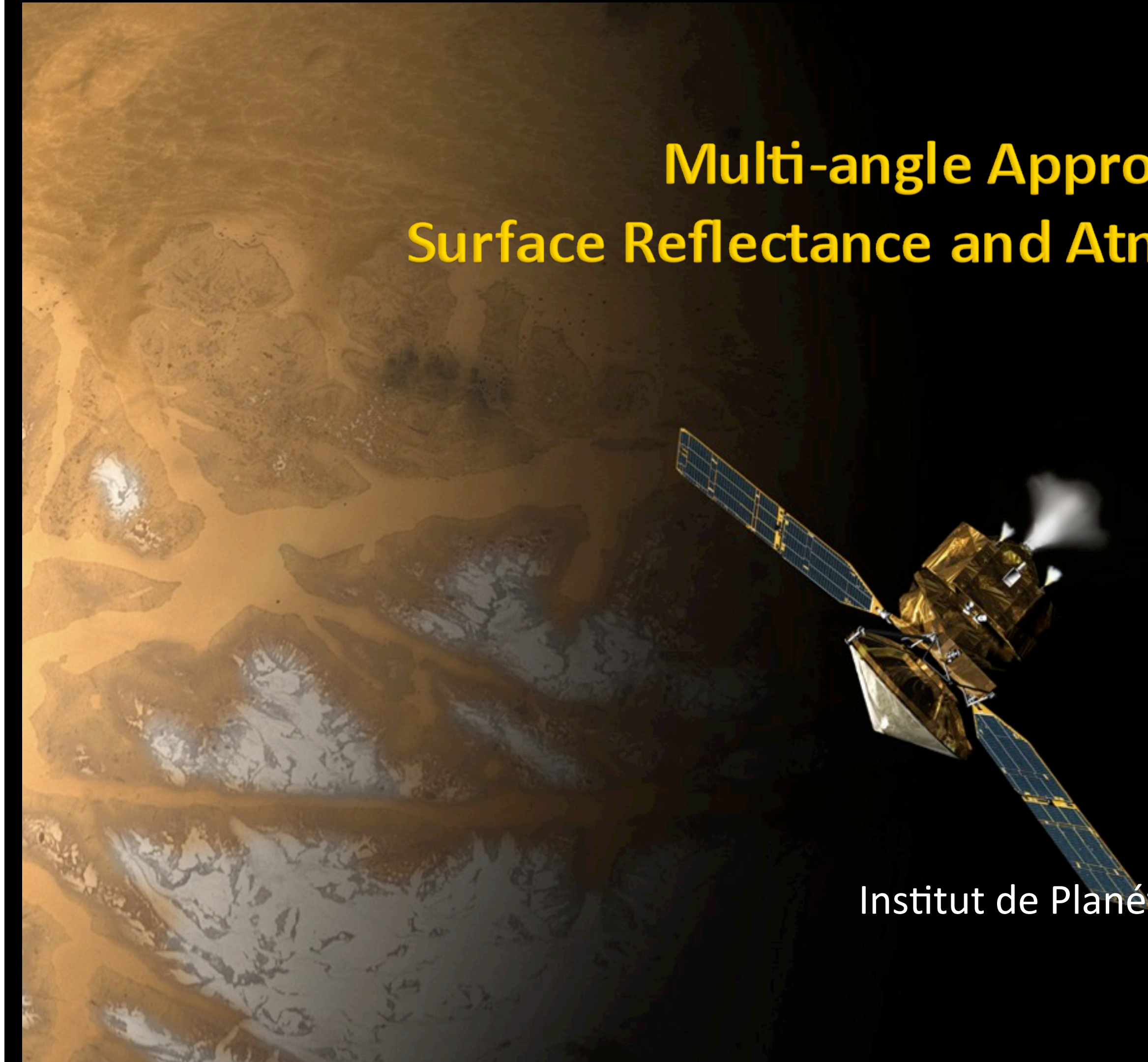

Mars-Reco III:

Multi-angle Approach for Coherent Retrieval of Surface Reflectance and Atmosphere Optical Depth from CRISM Observations

S. DOUTÉ

Institut de Planétologie et d'Astrophysique de Grenoble (IPAG)

X. Ceamanos

Météo-France/CNRS, CNRM/GAME, Toulouse

IPAG
Institut de Planétologie
et d'Astrophysique
de Grenoble

IPAG:

Funding :

Agence Nationale de la Recherche
ANR

PNTS

Outline

- Surface reflectance and Atmosphere Optical Depth
- Method for atmospheric correction
- Results and discussion

La reflectance de surface

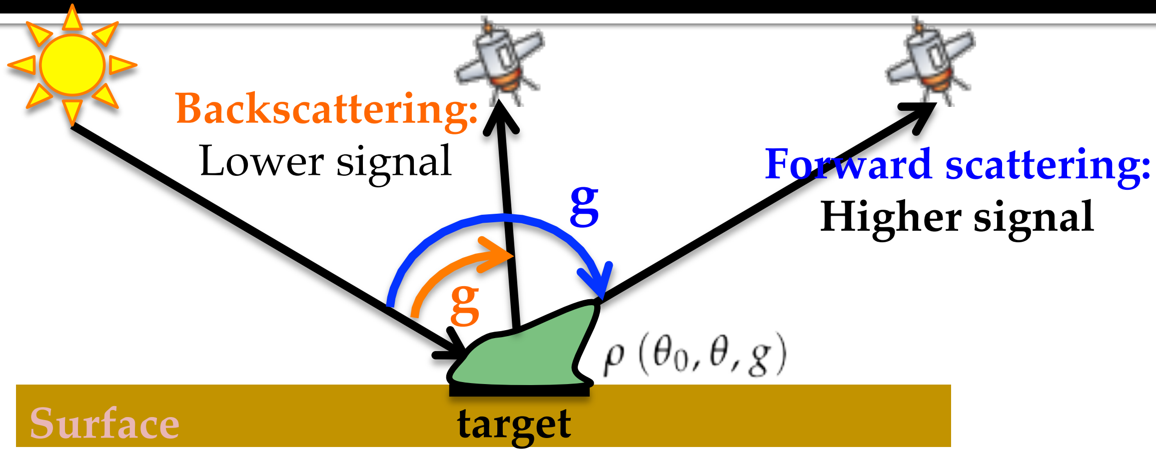

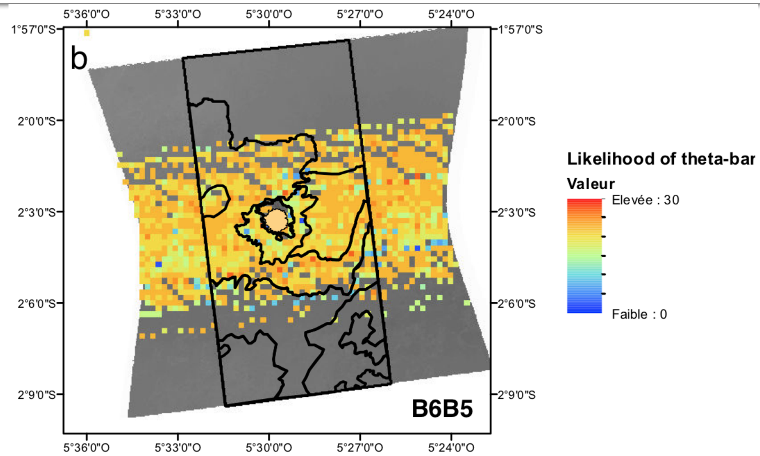

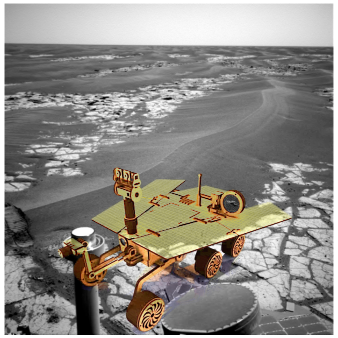

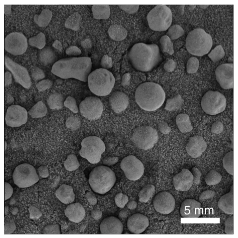

spherule soils

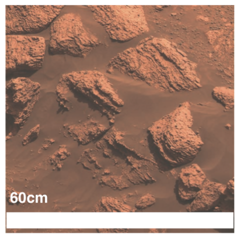

outcrops

Fernando et al. JGR 2013

- **BRDF(θ_0,θ,φ)**: bidirectional reflectance distribution function

  un paramètre clef pour

  - caractériser l'état physique des matériaux à la surface
  - corriger les effets atmosphériques précisément sur l'image haute résolution
  - effectuer le démélange spectral de l'image -> abondance des composants.

The atmosphere of Mars

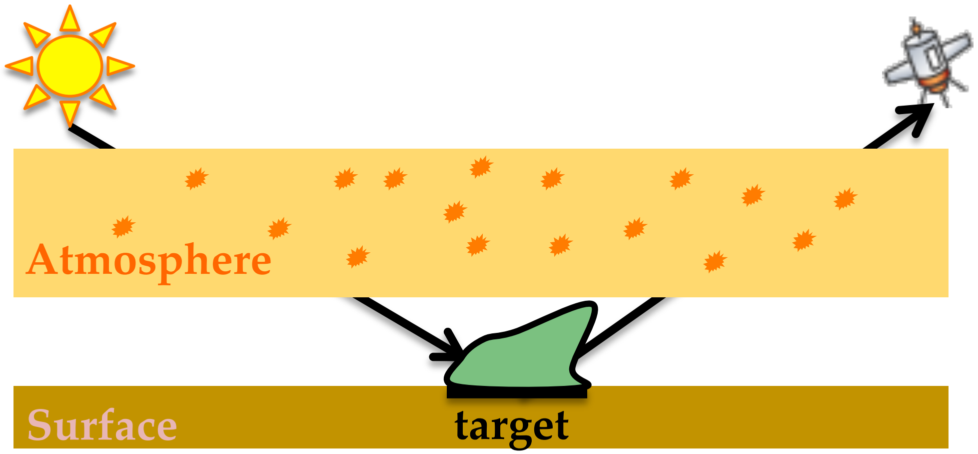

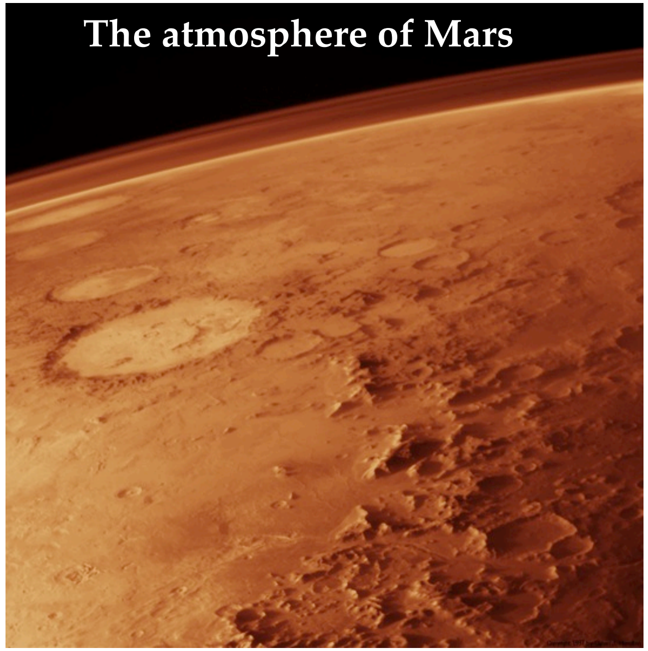

- Martian atmosphere
  - Faint but significant opacities
  - Conditions vary with time and space
  - Obstacle in sensing the surface!

The atmosphere of Mars

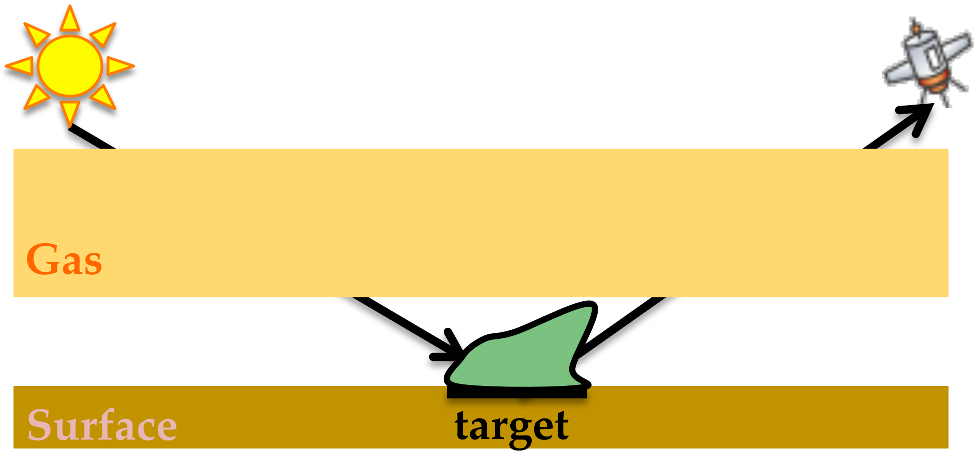

Vertical transmission spectrum of CO_2 gas in the SWIR

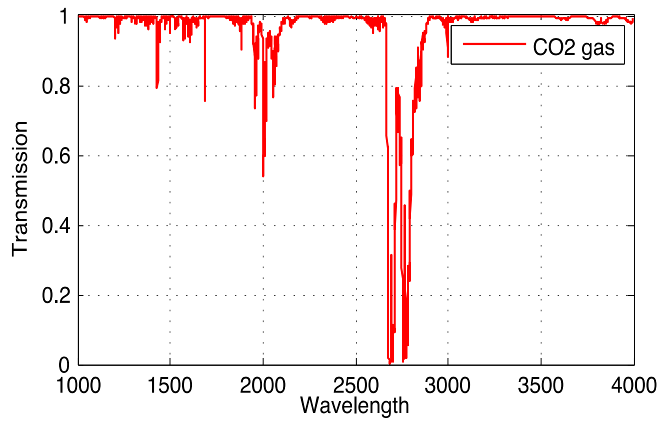

- Martian atmosphere
  - ① Gases
  - **Composition**: 95% CO_2
  - **Effect on surface reflectance**: multiplicative filter
  - **Correction**: calculation of vertical transmission spectrum [Langevin et al. 2005, McGuire et al. 2009, Douté 2009]

The atmosphere of Mars

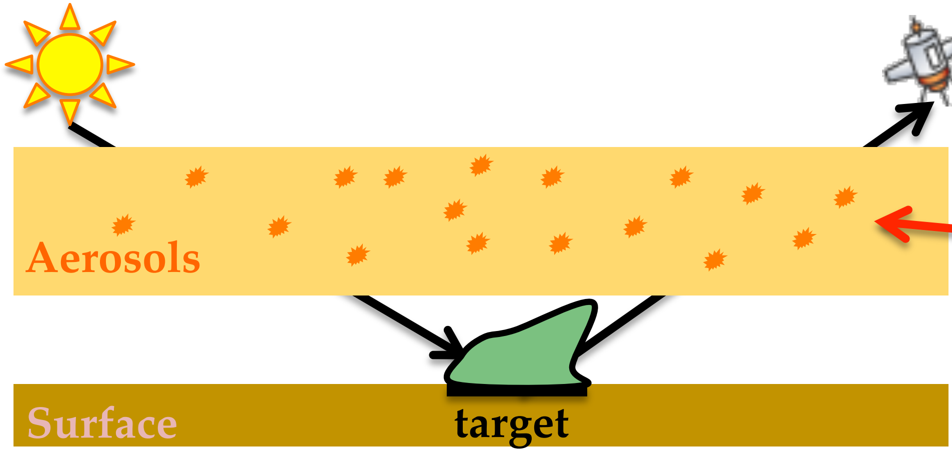

Variable aerosol content!

- Martian atmosphere
  - ② Aerosols
  - **Composition**: mineral and water ice particulates

The atmosphere of Mars

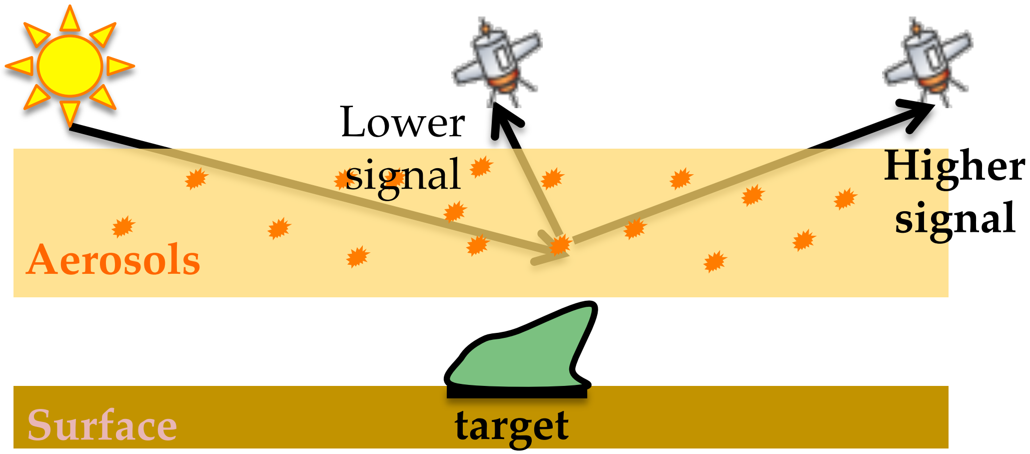

Martian dust aerosols phase function [Wolff 2009]

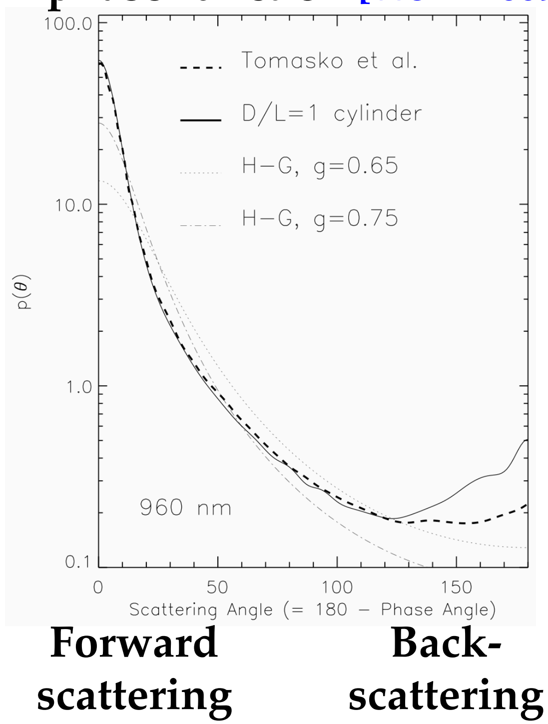

- Martian atmosphere
  - ② Aerosols
    - **Composition**: mineral and water ice particulates
    - **Effect on TOA reflectance**: anisotropic effect depending on geometry

The atmosphere of Mars

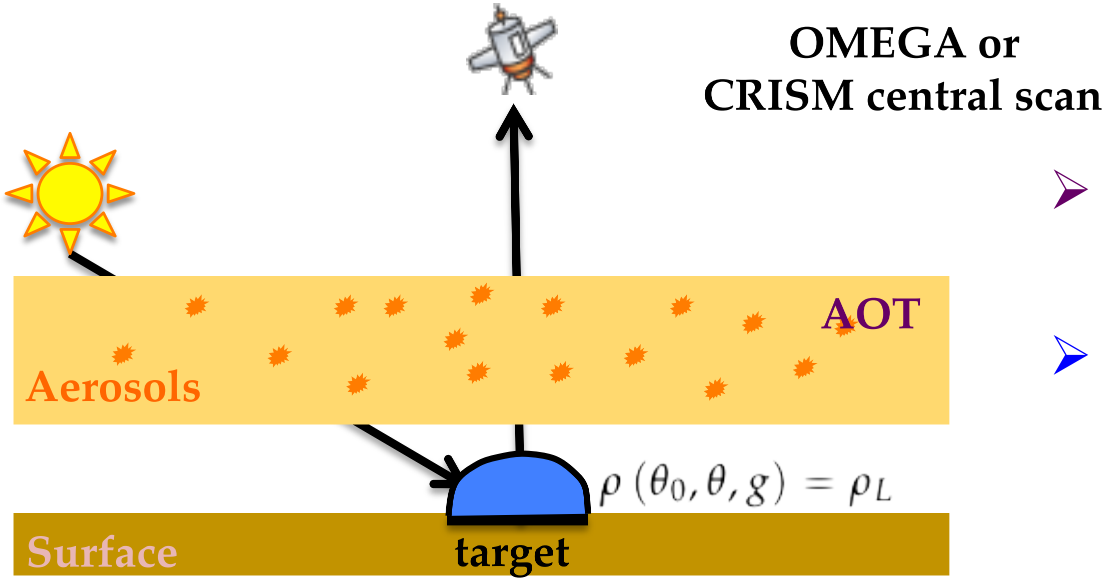

- **Aerosol optical thickness (AOT):** aerosol content
- **Lambertian assumption**: adopted for OMEGA observations and single-shot CRISM images

- Martian atmosphere
  - ② Aerosols
  - **Composition**: mineral and water ice particulates
  - **Effect on TOA reflectance**: anisotropic effect depending on geometry
  - **Correction**: content estimation + assumption on the surface scattering properties [Vincendon et al. 2007, McGuire et al. 2008, Cull et al. 2010]

The atmosphere of Mars

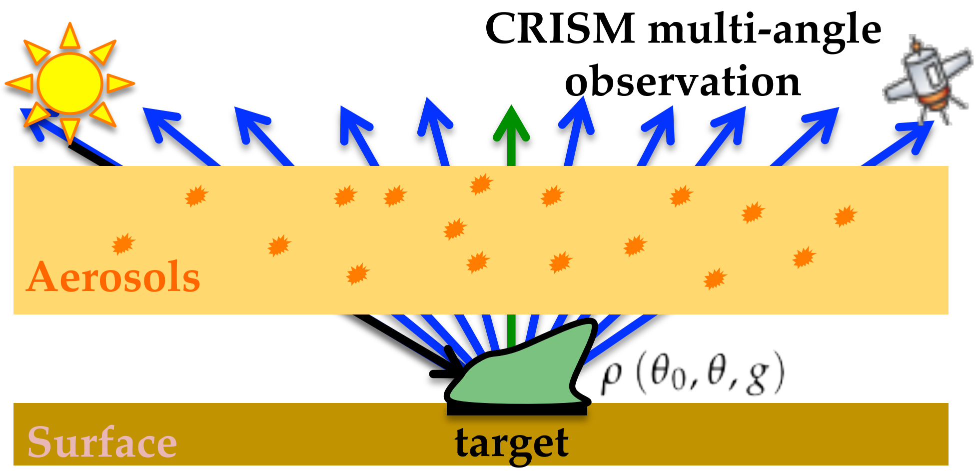

CRISM offers unprecedented data to compensate for atmospheric effects considering the anisotropy of the surface and of the aerosols!

- Martian atmosphere

  ② Aerosols

  - **Composition**: mineral and water ice particulates
  - **Effect on TOA reflectance**: anisotropic effect depending on geometry
  - **Correction**: content estimation + assumption on the surface scattering properties [Vincendon et al. 2007, McGuire et al. 2008, Cull et al. 2010]

CRISM: Compact Reconnaissance Imaging Spectrometer for Mars

- Quasi-nadir targeted **central scan**
  - Full spatial resolution (18 m/pix)
  - 544 channels
- **Emission Phase Function** (EPF)
  - Ten additional spatially binned scans (VZA < 70º, 180 m/pix)
  - 544 channels

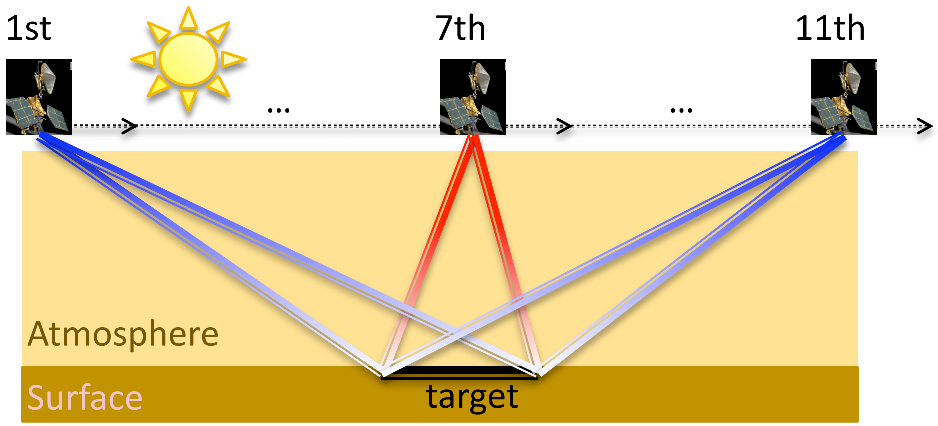

CRISM multi-angle observation

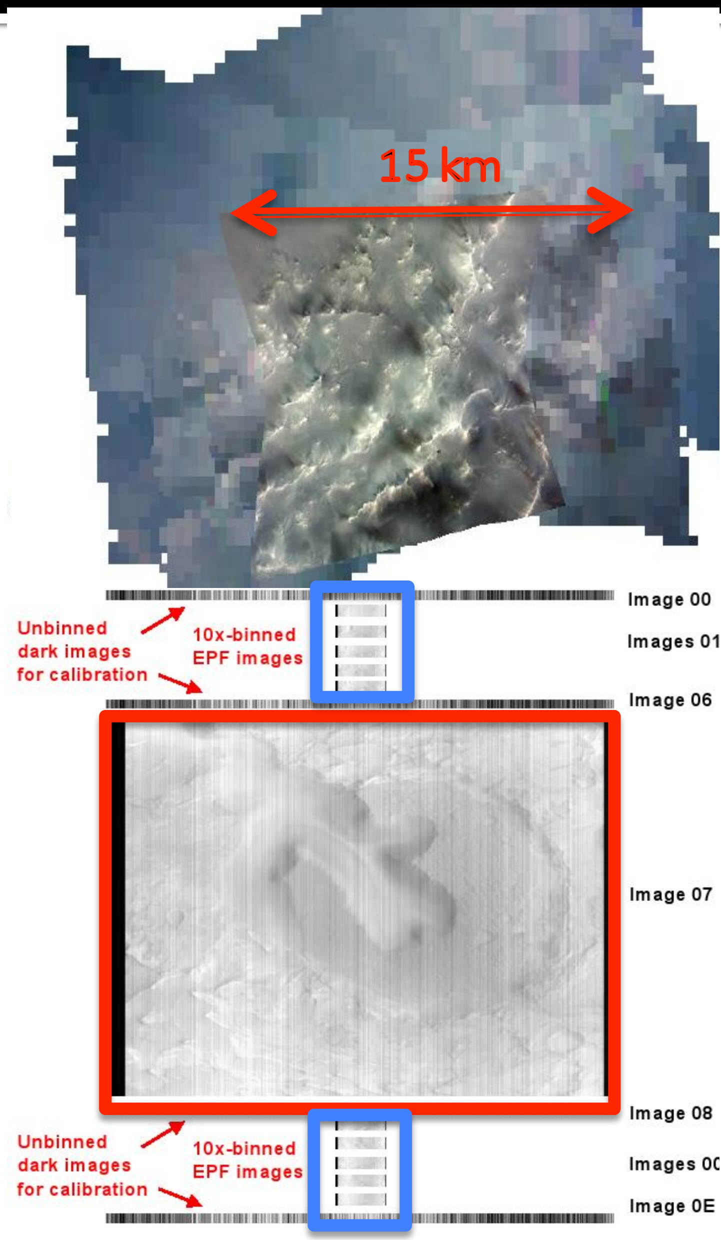

Outline

- Surface reflectance and

  Atmosphere Optical Depth
- Methods for atmospheric correction
- Results and discussion

Atmospheric correction

- Atmospheric correction chain for CRISM observations
  1. Generation of multi-angle product by data pipeline

CRISM targeted observation → Fusion of the 11 hyperspectral images → At-sensor photometric curves

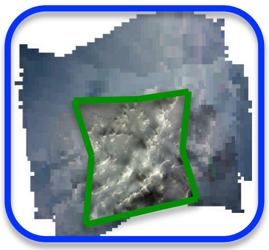

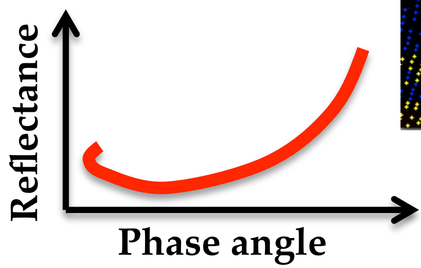

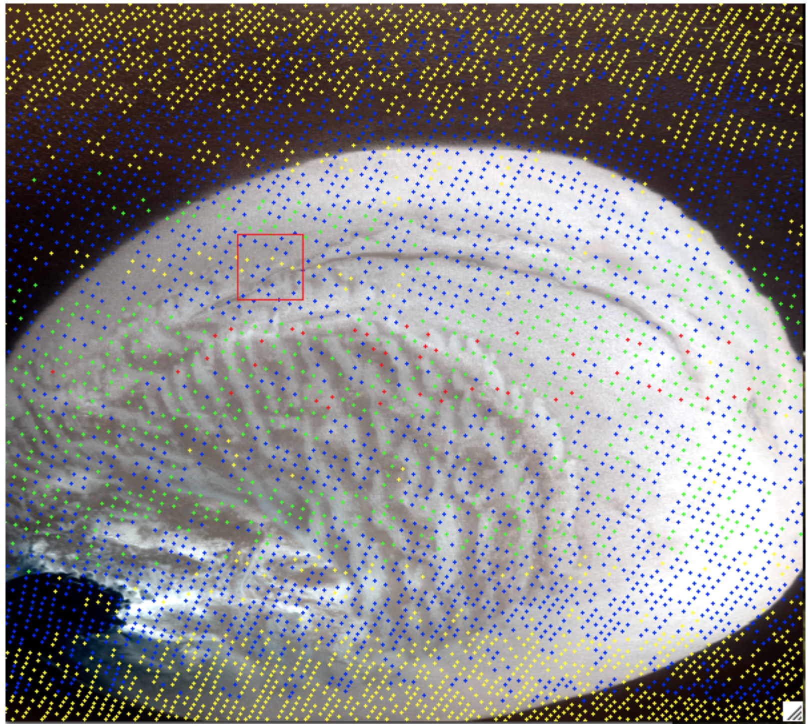

Atmospheric correction

- Atmospheric correction chain for CRISM observations
  1. Generation of multi-angle product by data pipeline
  2. Retrieval of aerosol optical thickness (AOT) [Douté 2010]

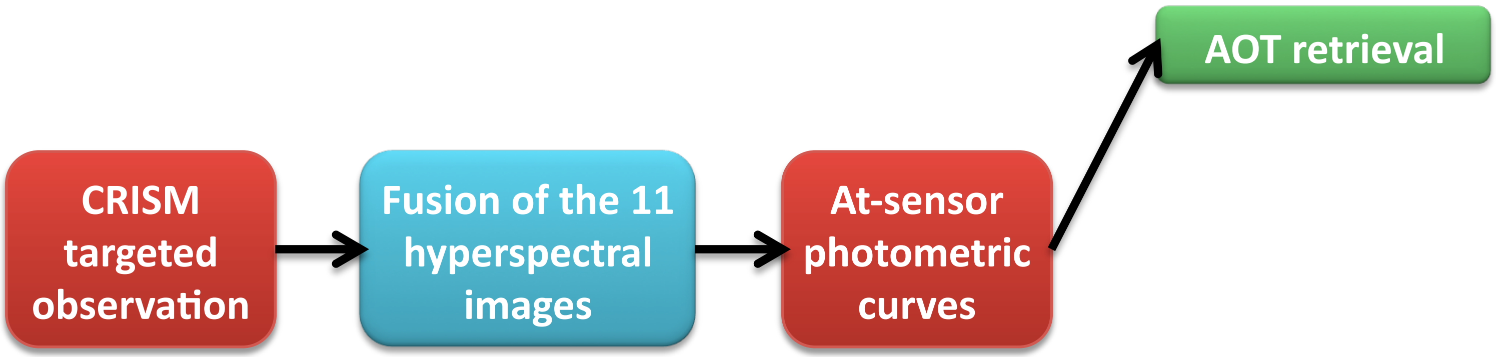

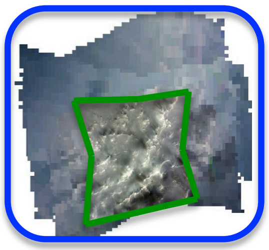

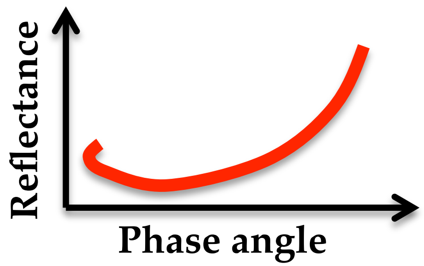

Atmospheric correction

- Atmospheric correction chain for CRISM observations
  1. Generation of multi-angle product by data pipeline
  2. Retrieval of aerosol optical thickness (AOT) [Douté 2010]
  3. Correction for gases [Douté 2009]

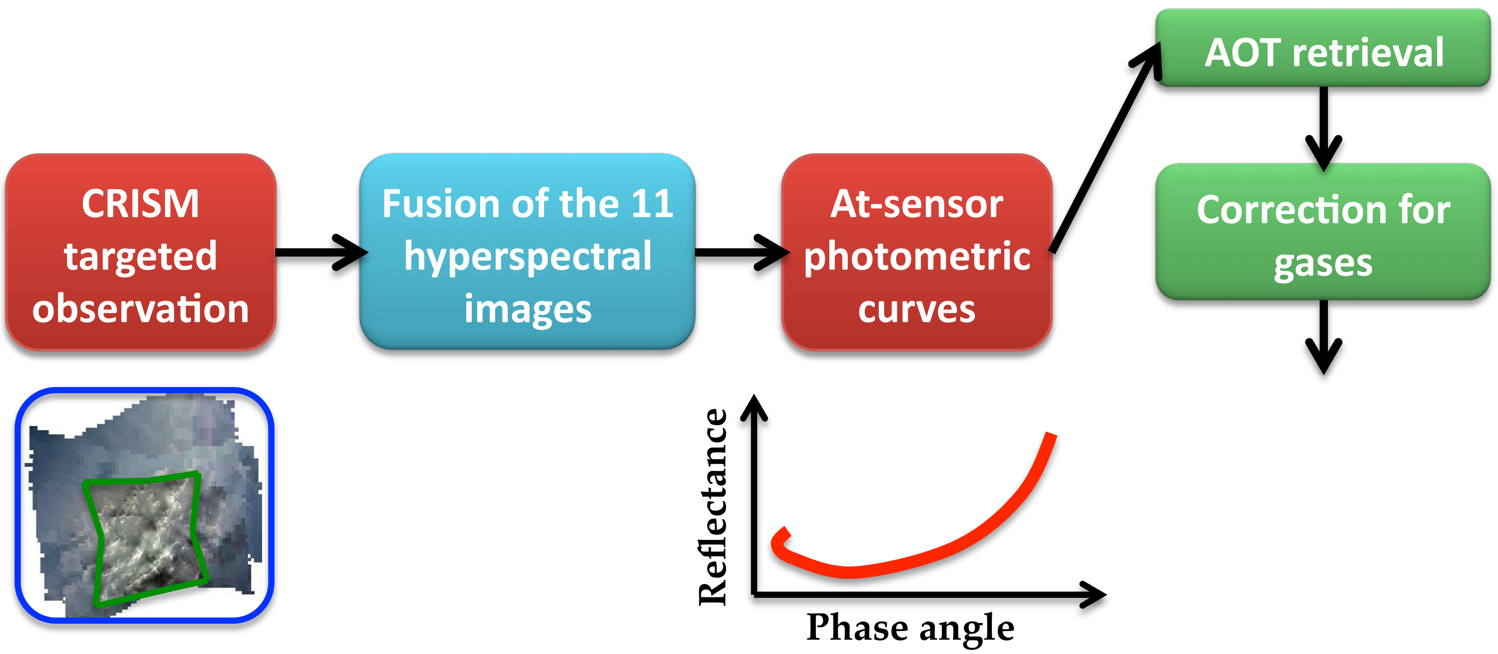

Atmospheric correction

- Atmospheric correction chain for CRISM observations
  1. Generation of multi-angle product by data pipeline
  2. Retrieval of aerosol optical thickness (AOT) [Douté 2010]
  3. Correction for gases [Douté 2009]
  4. Correction for aerosols: MARS-ReCO

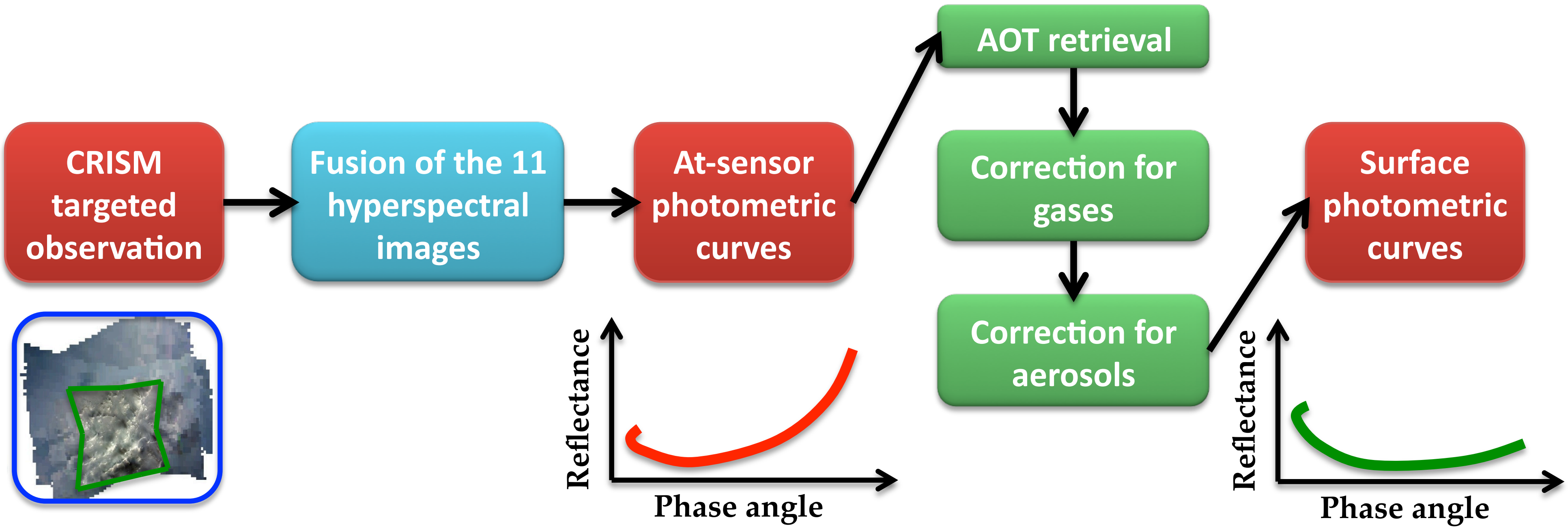

Atmospheric correction

- **MARS-ReCO III** Multi-angle Approach for Coherent Retrieval of Surface Reflectance and Atmosphere Optical Depth from CRISM Observations
  - considering the anisotropic scattering properties of the surface
  - inspired by work done on Earth observation [Carrer et al. 2010, Lyapustin 2011]
  - as a function of wavelength

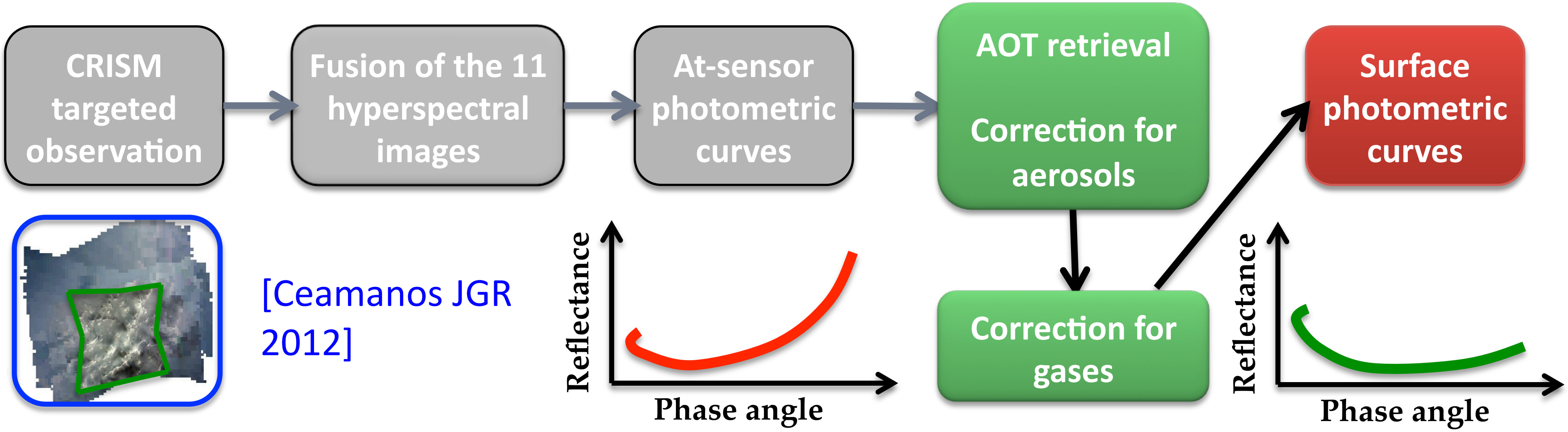

Surface scattering model

Surface anisotropy taken into account through its BRF expressed using a semi-empirical Ross-Thick Li-Sparse (RTLS) model

$$\rho\left(\mu_0,\mu,\varphi\right)=k^L+k^G f_G\left(\mu_0,\mu,\varphi\right)+k^V f_V\left(\mu_0,\mu,\varphi\right)$$

subscripts refer to Lambertian (*L*), geometric (*G*) and volumetric (*V*) components

f_G, f_V predefined geometric kernels.

This model has proved to be accurate in recreating many types of natural surface

Expression for the TOA reflectance

L can be decomposed as a sum of the atmospheric path radiance (*D*), and the radiance reflected by the surface before being directly (L_s) and diffusely (L_s^d) transmitted through the atmosphere:

$$L(s_0, s) = D(s_0, s) + L_s(s_0, s)e^{-\tau/|\mu|} + L_s^d(s_0, s)$$

surface-reflected radiance

$$L_s(s_0, s) \cong S\mu_0 e^{-\tau/\mu_0} \{\rho(s_0, s) + \alpha c_0 \rho_1(\mu)\rho_2(\mu_0)\} + \frac{\alpha}{\pi}\int_{\Omega+} D_s(s_0, s')\rho(s', s)\mu' ds'$$

ρ bidirectional reflectance factor (BRF)

c_0 spherical albedo of the atmosphere

α multiple reflection factor

ρ_1 ρ_2 hemispherical-directional albedos

D_s diffuse illumination at the surface

The diffusely transmitted surface-reflected radiance at the TOA is calculated from L_s with the help of one-dimensional diffuse Green's function of the atmosphere (G^d):

$$L_s^d(s_0, s) = \int_{\Omega^-} G^d(s_1, s) L_s(s_0, s_1) ds_1$$

The substitution of the RTLS model into the previous equations provides a quasi-linear expression of the TOA reflectance :

$$R\left(\mu_o, \mu, \varphi\right) = k^T R^D \left(\mu_o, \mu, \varphi\right) + k^L F^L \left(\mu_o, \mu\right) + k^G F^G \left(\mu_o, \mu, \varphi\right) + k^V F^V \left(\mu_o, \mu, \varphi\right) + R^{nl} \left(\mu_o, \mu\right)$$

$R^D \quad \left\{F^L, F^G, F^V\right\}$ surface-independent radiometric quantities

R^{nl} surface dependent nonlinear term

framework : a single-layer homogeneous atmosphere of mineral aerosols

Inversion strategy for surface reflectance

Atmospheric correction of each TOA photometric curve

$$\mathbf{R}^C = \{R_1^C, \ldots, R_{Ng}^C\}$$

N_g is the number of available angular measurements

$\mathbf{k}_{sol}$ Solution for the RTLS kernel weights + AOD $\{k^L, k^G, k^V, k^T\}$

that provide the best fit between the observed data $\mathbf{R}^C$

and the predicted photometric curve $\mathbf{R} = \{R_1, \ldots, R_{Ng}\}$

An iterative inversion strategy is proposed based on a formalism which integrates several sources of uncertainty in the inversion process and propagates them to the solution.

Iterative inversion

On the first iteration :

MARS-ReCO assumes an isotropic surface

$$\mathbf{k}^{(0)} = \{R^C_{bck}, 0, 0, \tau_{guess}\}$$

a set of reduced observables

$$\mathbf{r}^{(0)} = \left\{r_1^{(0)}, \ldots r_{Ng}^{(0)}\right\}$$

where $r_j^{(0)} = R_j - R_j^{nl(0)}$

the quantity $R_j^D(k^{T(0)}) + R_j^{nl}(\mathbf{k}^{(0)})$ can be computed, knowing $\mathbf{k}^{(0)}$

and using the LUT's.

The model relating the state vector ***k*** to the measurements ***R*** is quasi-linear:

$$\mathbf{r}^{(0)} = \mathbf{G}^{(0)}\mathbf{k}, \quad \mathbf{G}^{(0)} = \begin{bmatrix} F_1^{L(0)} & F_1^{G(0)} & F_1^{V(0)} & R_1^{D(0)} \\ & \cdots & & \\ F_j^{L(0)} & F_j^{G(0)} & F_j^{V(0)} & R_j^{D(0)} \\ & \cdots & & \\ F_{N_g}^{L(0)} & F_{N_g}^{G(0)} & F_{N_g}^{V(0)} & R_{N_g}^{D(0)} \end{bmatrix}$$

Characterizing the uncertainties

A set of Gaussian probability distribution functions (PDFs) express the state of information pertaining to the input and output parameters of the inversion problem:

1. error on the CRISM measurements R_j^C caracterized by the diagonal covariance matrix $\mathbf{C}_C$ with elements $\sigma_1^2, \ldots, \sigma_{N_g}^2$
2. error on the AOT estimation τ which induces an error on $R_j^D + R_j^{nl(0)}$ for each geometry $j = 1, \ldots, N_g$. Elements of the covariance matrix $\mathbf{C}_\tau^{(0)}$ evaluated experimentally.
3. total covariance matrix for the reduced measurements $\mathbf{C}_r^{(0)} = \mathbf{C}_C + \mathbf{C}_\tau^{(0)}$
4. a priori information on the kernel weights: mean $\mathbf{k}^{(0)}$ and a covariance matrix $\mathbf{C}_k$

Retrieval of surface reflectance and propagation of errors

most likely a posteriori :

weight vector $\boldsymbol{k}^{(1)}$

covariance matrix $\mathbf{C}_{kp}$ (associated to $\boldsymbol{k}^{(1)}$)

covariance matrix $\mathbf{C}_{rp}$ (associated to the model of TOA reflectance)

retrieved through the explicit least-squares solution:

$$\mathbf{k}^{(1)} = \mathbf{k}^{(0)} + \mathbf{C}_k \mathbf{G}^{(0)T} \left(\mathbf{G}^{(0)} \mathbf{C}_k \mathbf{G}^{(0)T} + \mathbf{C}_r^{(0)} \right)^{-1} \left(\mathbf{r}^{(0)} - \mathbf{G}^{(0)} \mathbf{k}^{(0)} \right),$$

$$\mathbf{C}_{kp} = \mathbf{C}_k - \mathbf{C}_k \mathbf{G}^{(0)T} \left(\mathbf{G}^{(0)} \mathbf{C}_k \mathbf{G}^{(0)T} + \mathbf{C}_r^{(0)} \right)^{-1} \mathbf{G}^{(0)} \mathbf{C}_k,$$

$$\mathbf{C}_{rp} = \mathbf{G}^{(0)} \mathbf{C}_{kp} \mathbf{G}^{(0)T} + \mathbf{C}_{AOT}^{(0)}.$$

retrieved vector $\boldsymbol{k}^{(1)}$ provides a refined estimate of

- the surface BRF
- the model $\mathbf{G}^1$
- the reduced observables $\mathbf{r}^{(1)}$ and $\mathbf{C}_r^{(1)}$

Convergence scheme

Properties of the atmosphere more stationary than the surface
the spatial or (spectral) dimension is exploited for simultaneous retrieval of the surface BRDF and atmospheric opacity.

Iterative inversion procedure, perpetuated using a Kalman filter

regularization procedure

$$C_k = \left(C_x^{-1} + C_{reg}^{-1}\right)^{-1}$$

$$k^{(0)} = C_k \left(C_x^{-1} k_p + C_{reg}^{-1} k_{reg}\right)$$

a prognostic model operator to calculate the prior $\mathbf{C_x}$ and $\mathbf{k_p}$ for super-pixel J considering the solution for super-pixel J-1 :

$$kp = k_{sol}$$

$$Ck = (1 + \delta)\mathrm{diag}(\mathrm{C_{kp}})$$

where $\mathrm{k_{sol}}$ and $\mathbf{C_{kp}}$ are related to iteration J-1

The transition probabilities for the variances are described by vector :

$$\delta = \left(2^{2/t_1} - 1,\ 2^{2/t_2} - 1,\ 2^{2/t_3} - 1,\ 2^{2/t_4} - 1\right)$$

Numerical experiments

Inversion parameters :
$\boldsymbol{k}_{reg}$=[0 0.03 0.02 0]
$\boldsymbol{C}_{reg}$=diag([10, 0.05 0.5 50])

The characteristic "times" (going from one super-pixel to the next) for the transition are t1=2; t2=10; t3=10; for the surface model and is variable for the AOD depending on the number of valid geometries

The more reduced the number of valid geometries, the smaller is the transition probability for the AOD variance and the more constrained is the AOD

We have conducted a test of our method and an intercomparison with other methods on a series of CRISM observations.

Outline

- Surface reflectance and Atmosphere Optical Depth
- Methods for atmospheric correction
- Tests and discussion

FRT3192

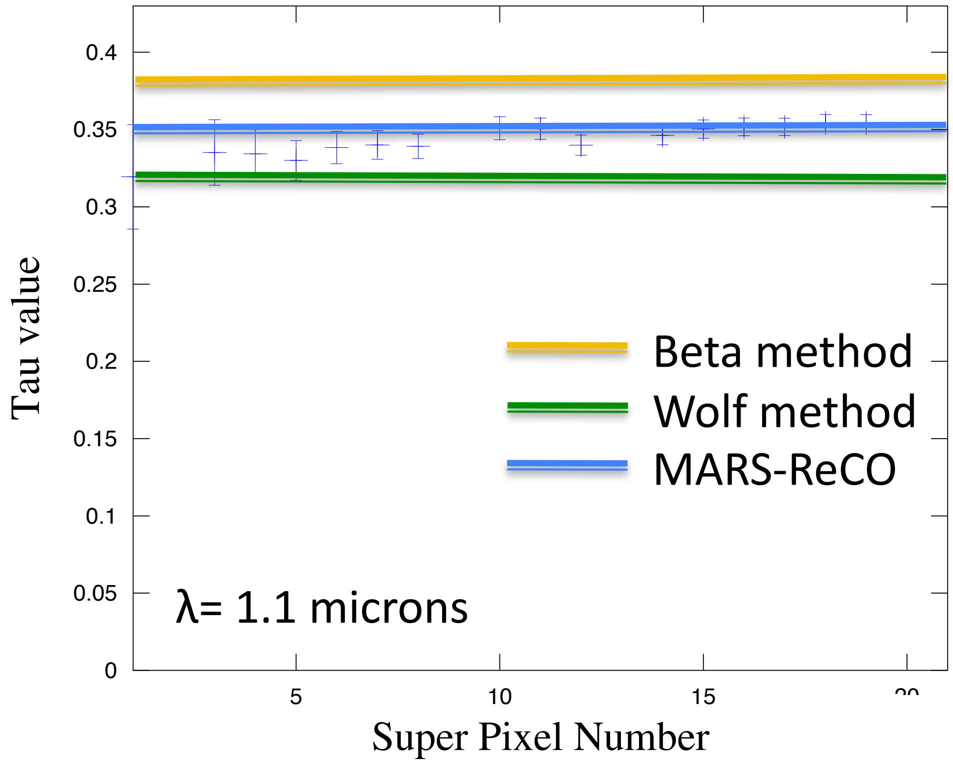

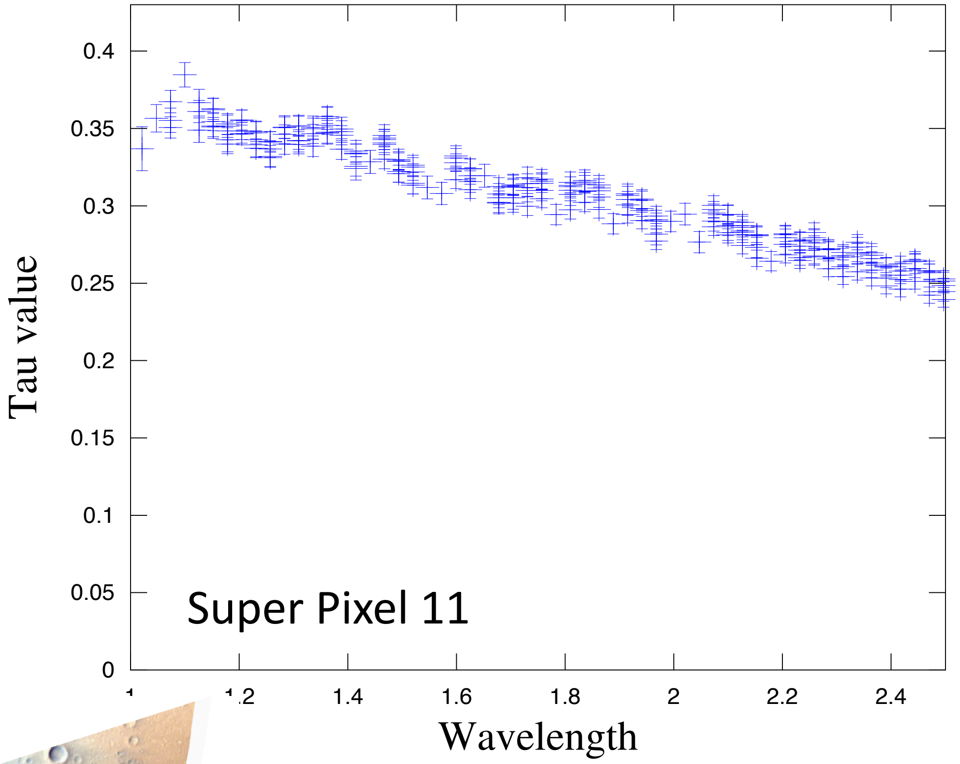

phase=56-112°

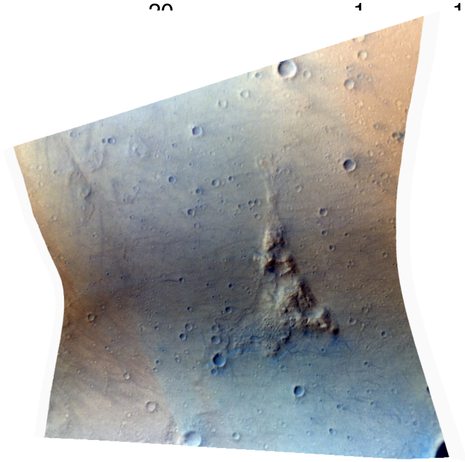

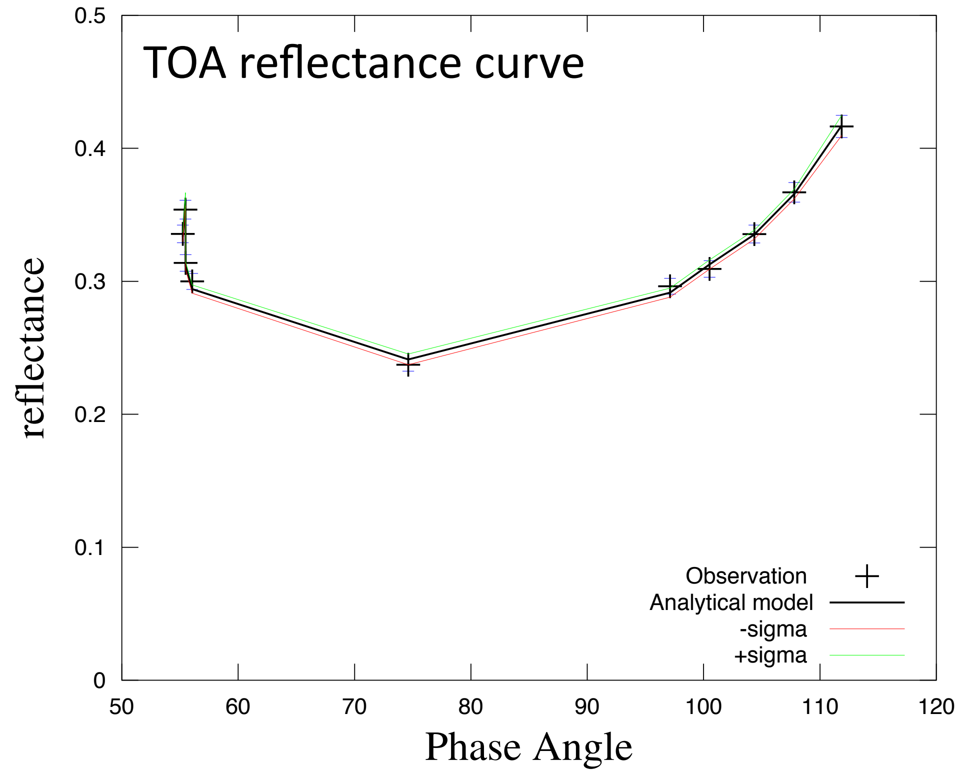
TOA reflectance curve
reflectance
Phase Angle
0
0.1
0.2
0.3
0.4
0.5
50
60
70
80
90
100
110
120
Observation
Analytical model
-sigma
+sigma

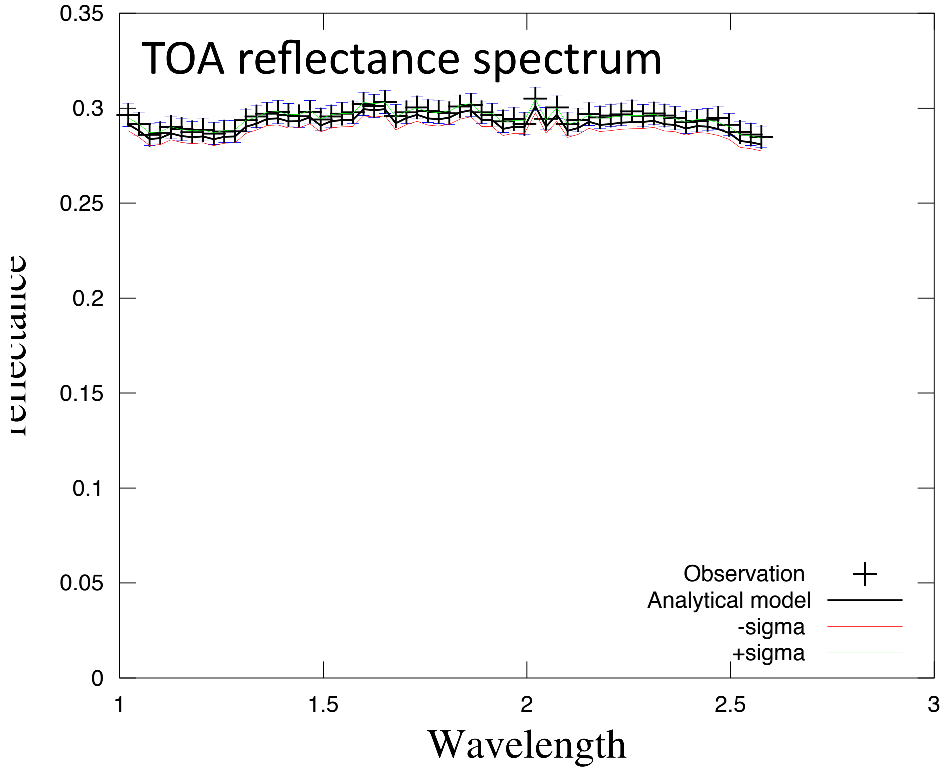
TOA reflectance spectrum
Wavelength
0
0.05
0.1
0.15
0.2
0.25
0.3
0.35
1
1.5
2
2.5
3
Observation
Analytical model
-sigma
+sigma

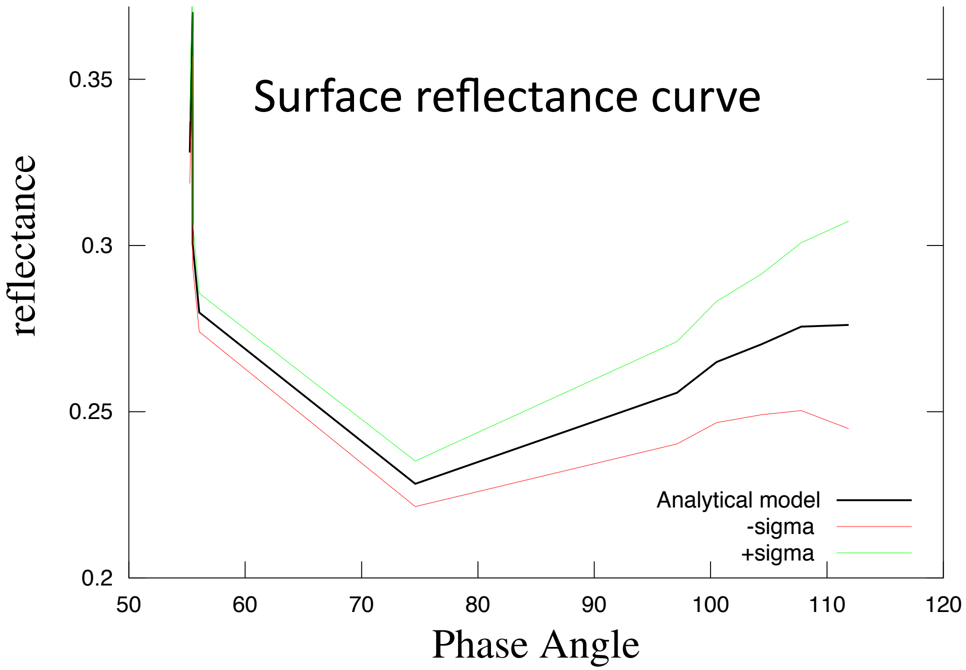
Surface reflectance curve
reflectance
Phase Angle
0.2
0.25
0.3
0.35
50
60
70
80
90
100
110
120
Analytical model
-sigma
+sigma

FRTCDA5

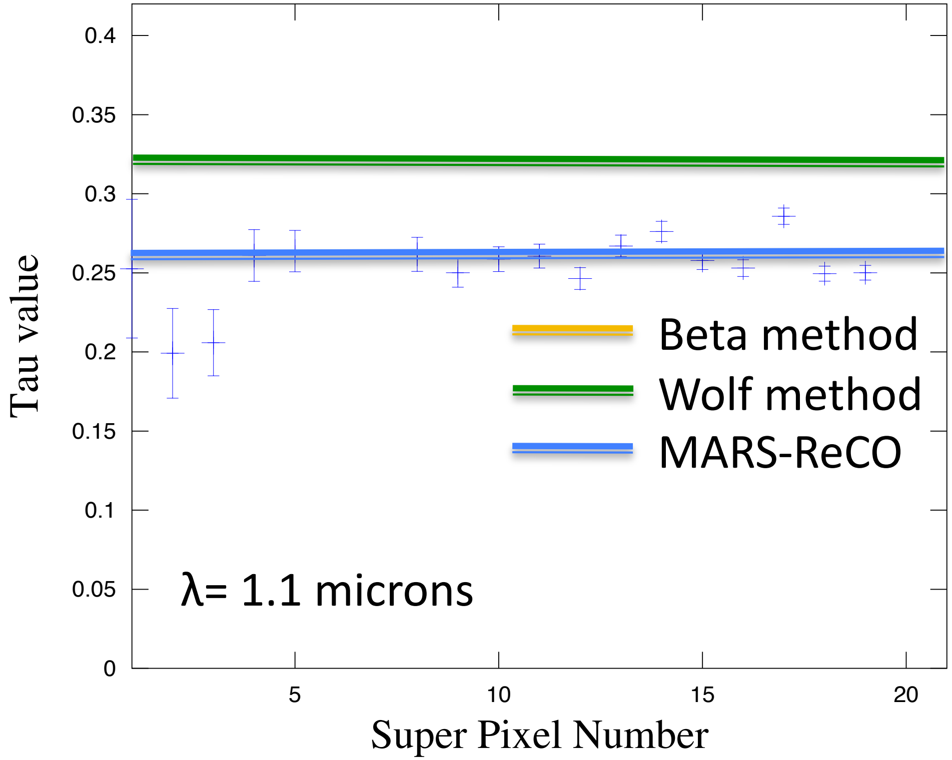

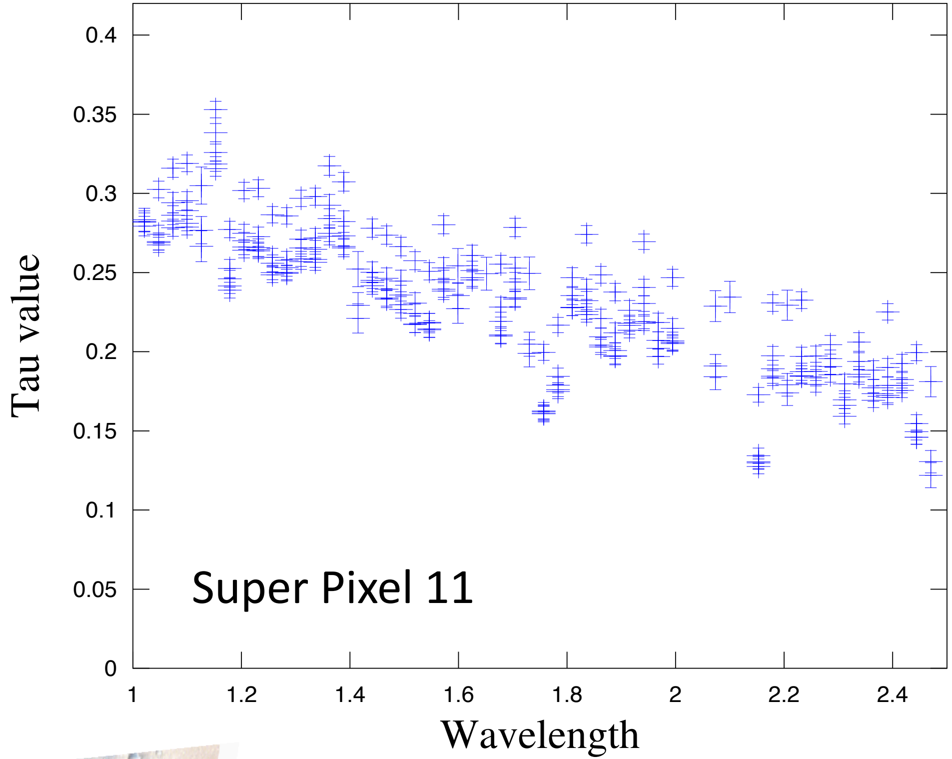

phase=46-106°

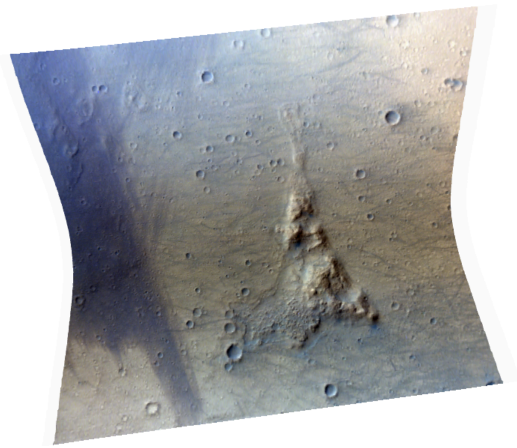

FRT8CE1

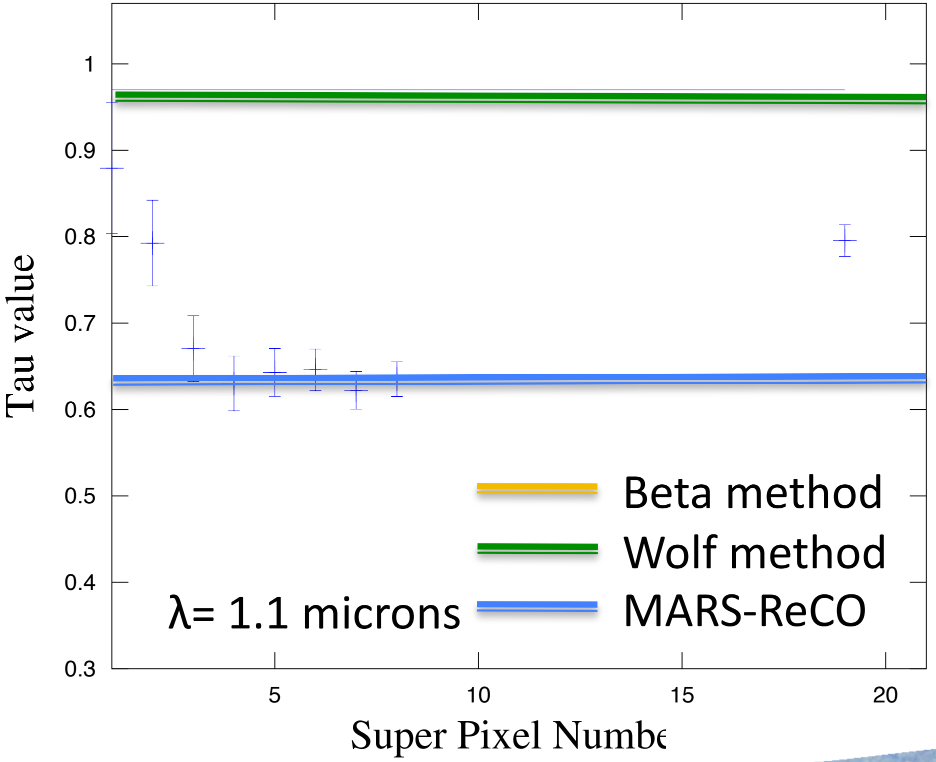

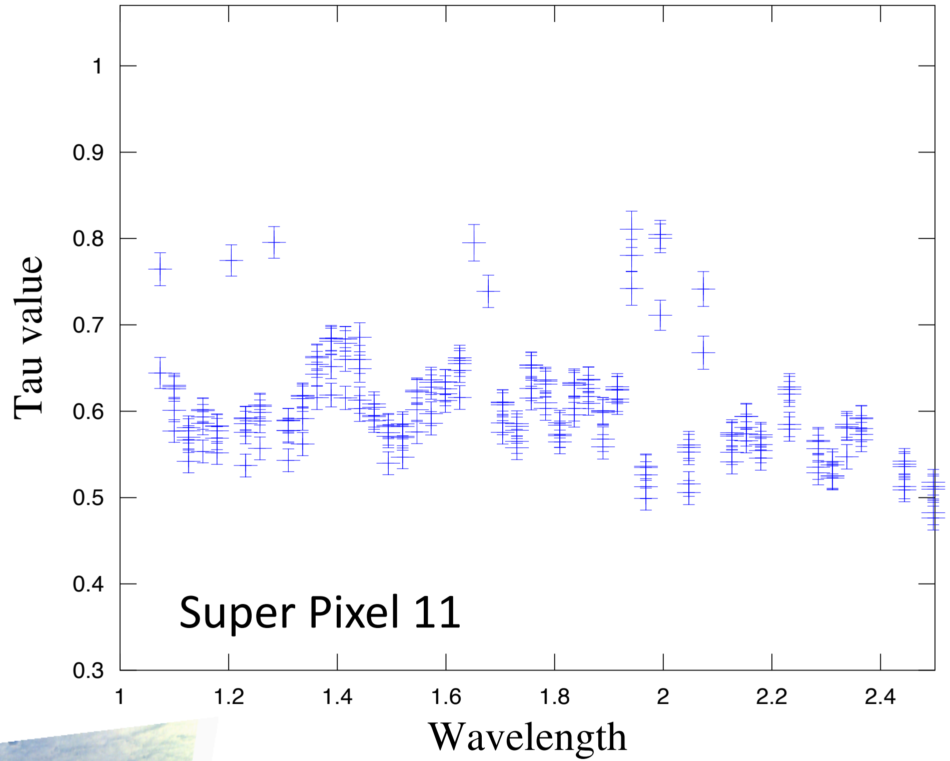

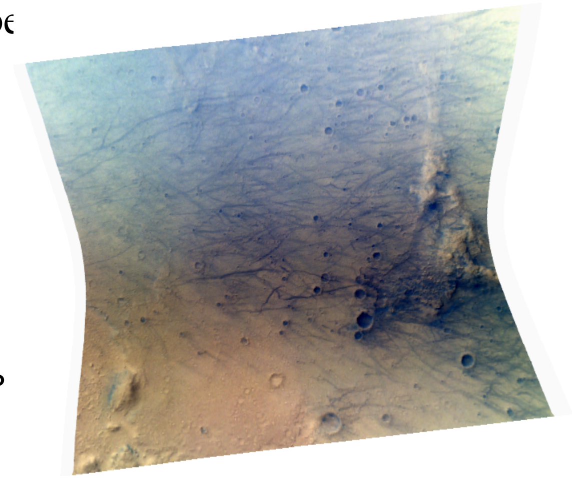

phase=41-90°

FRT63B0

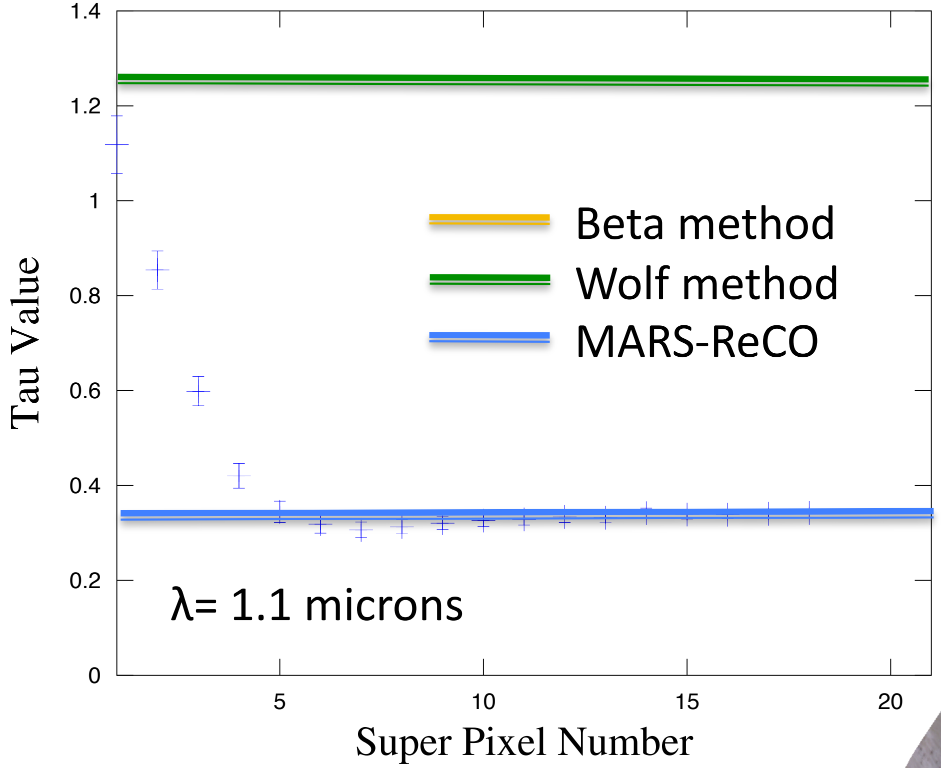

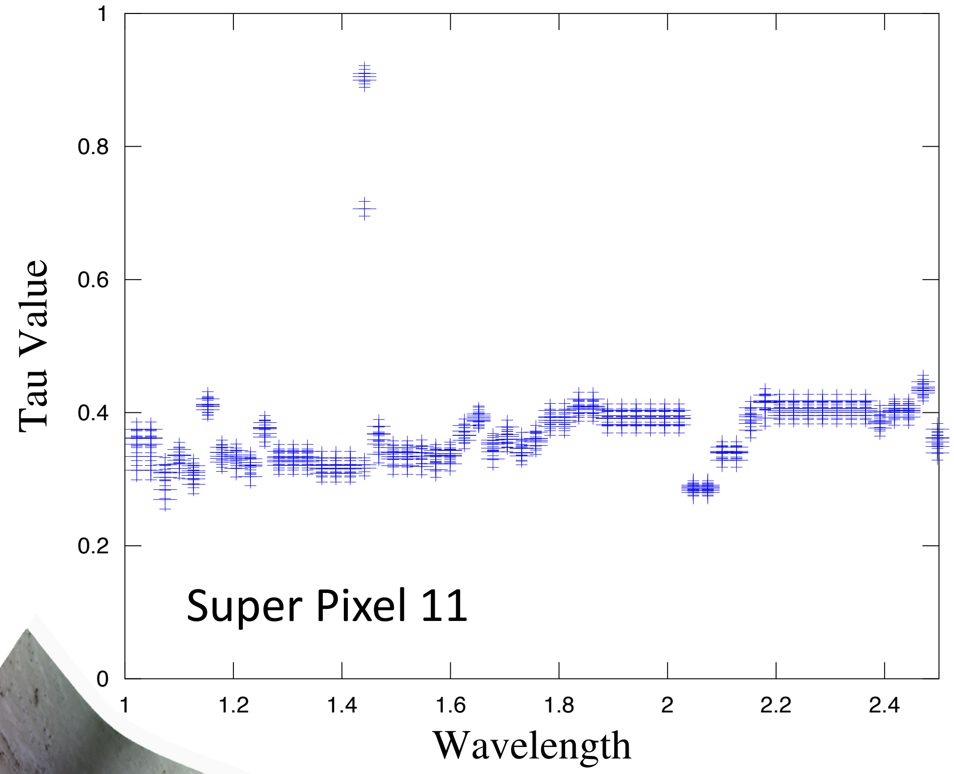

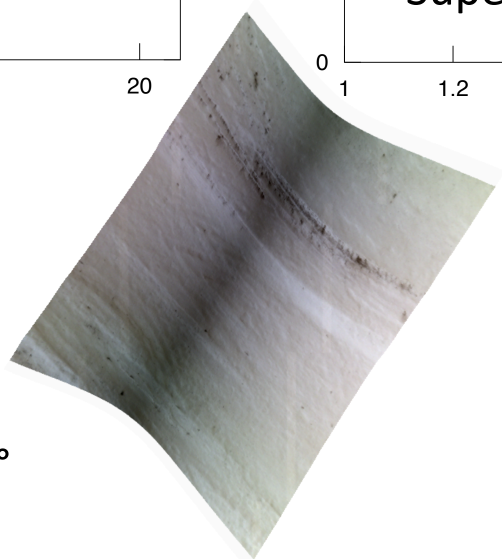

phase=40-115°

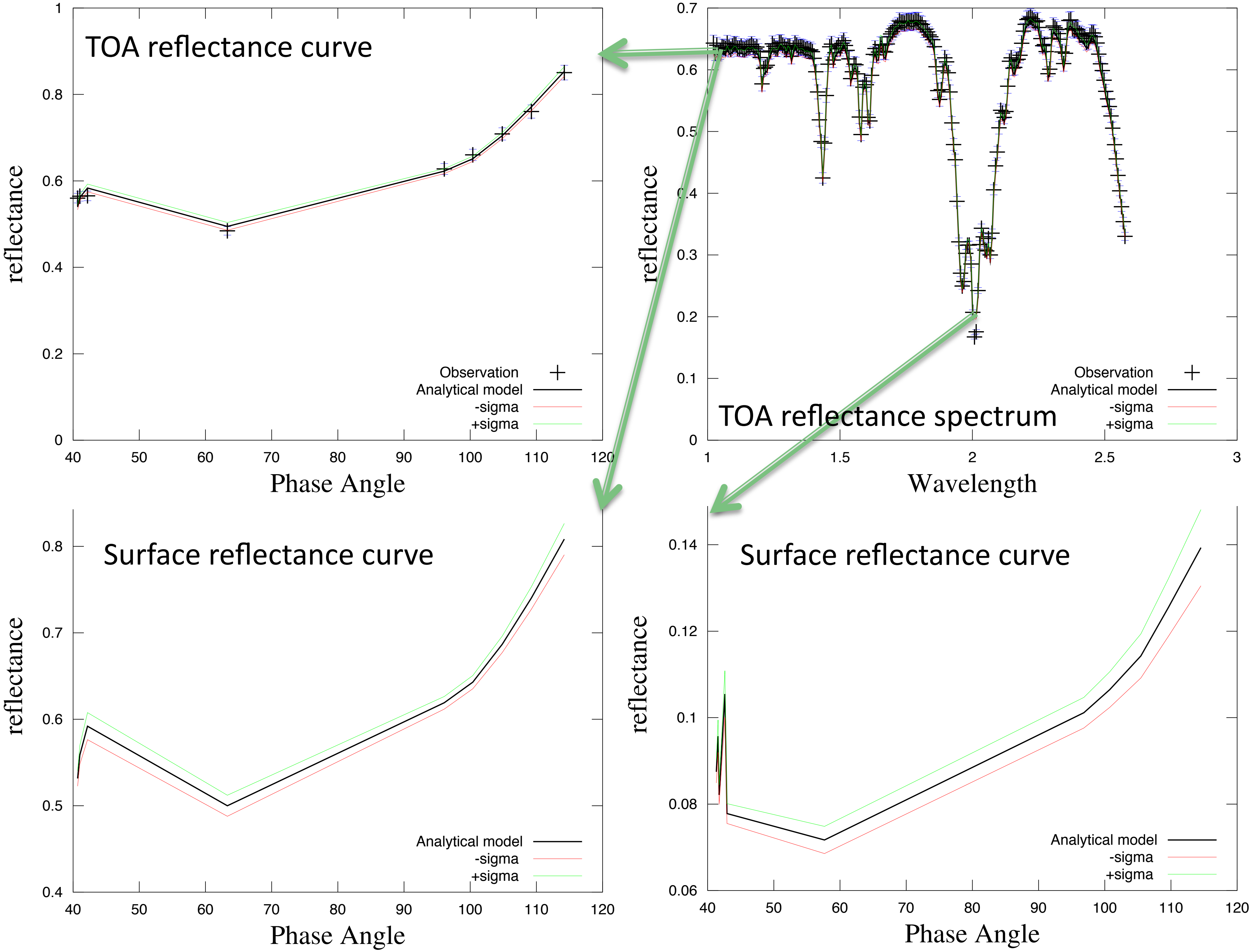
TOA reflectance curve
reflectance
Phase Angle
0
0.2
0.4
0.6
0.8
1
40
50
60
70
80
90
100
110
120
Observation
Analytical model
-sigma
+sigma
TOA reflectance spectrum
reflectance
Wavelength
0
0.1
0.2
0.3
0.4
0.5
0.6
0.7
1
1.5
2
2.5
3
Observation
Analytical model
-sigma
+sigma
Surface reflectance curve
reflectance
Phase Angle
0.4
0.5
0.6
0.7
0.8
40
50
60
70
80
90
100
110
120
Analytical model
-sigma
+sigma
Surface reflectance curve
reflectance
Phase Angle
0.06
0.08
0.1
0.12
0.14
40
50
60
70
80
90
100
110
120
Analytical model
-sigma
+sigma

FRT2F70

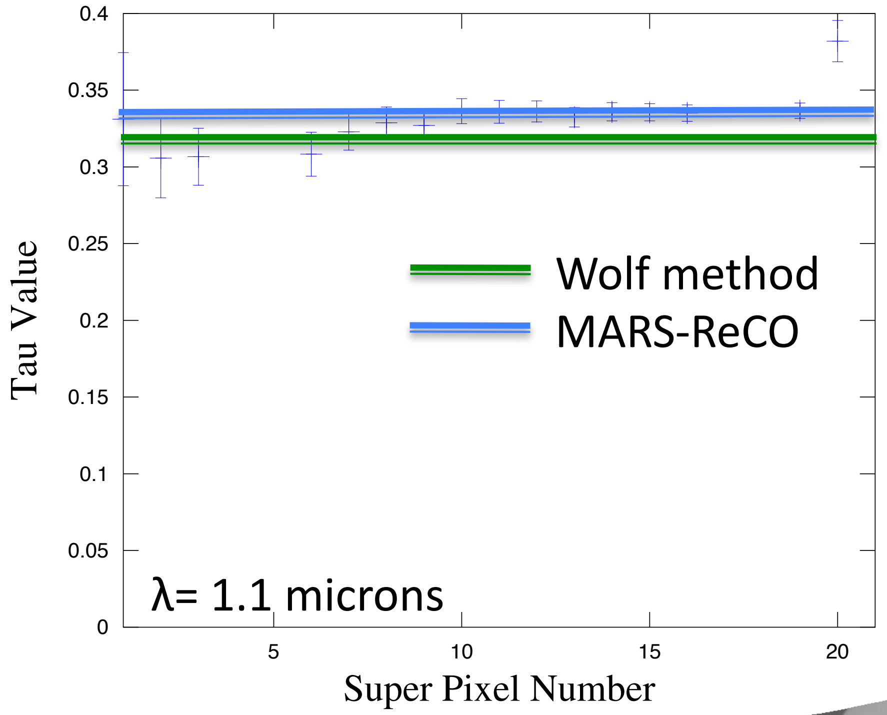
0.4
0.35
0.3
0.25
0.2
0.15
0.1
0.05
0
Tau Value
5
10
15
20
Super Pixel Number
Wolf method
MARS-ReCO
λ= 1.1 microns

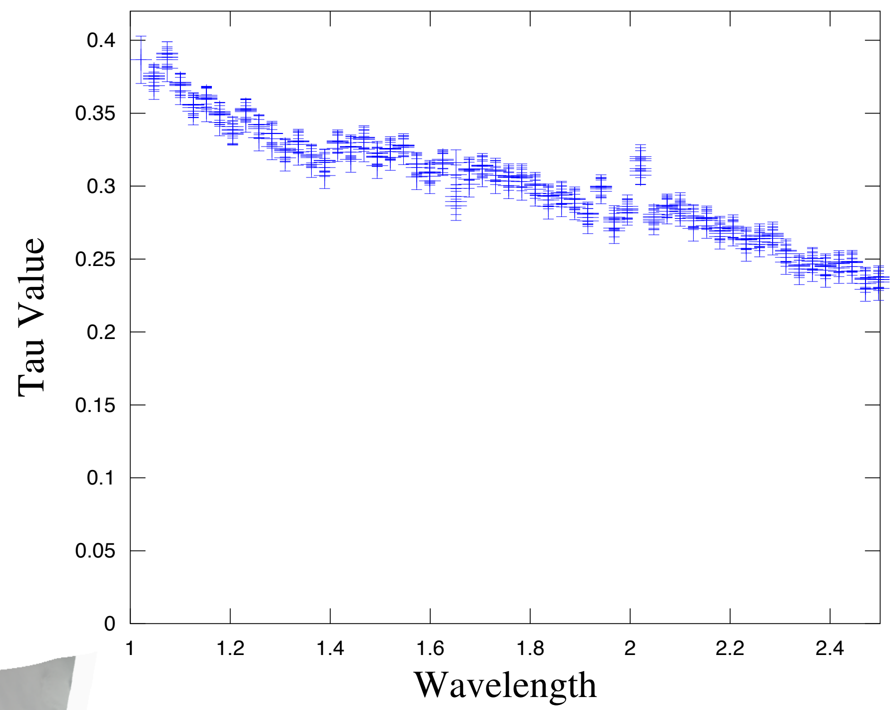
0.4
0.35
0.3
0.25
0.2
0.15
0.1
0.05
0
Tau Value
1
1.2
1.4
1.6
1.8
2
2.2
2.4
Wavelength

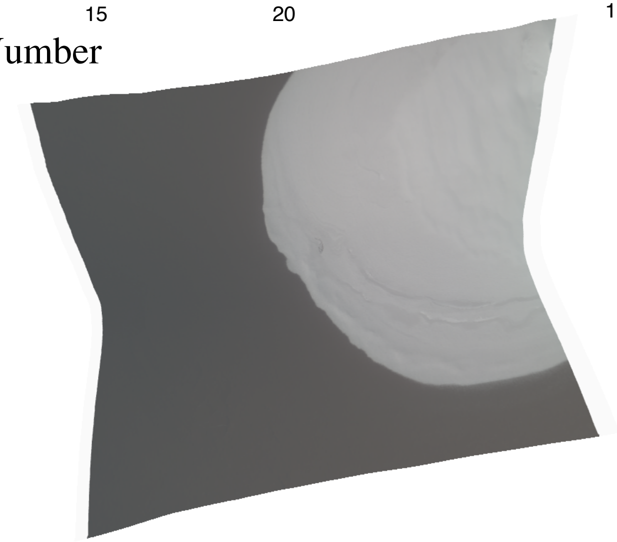

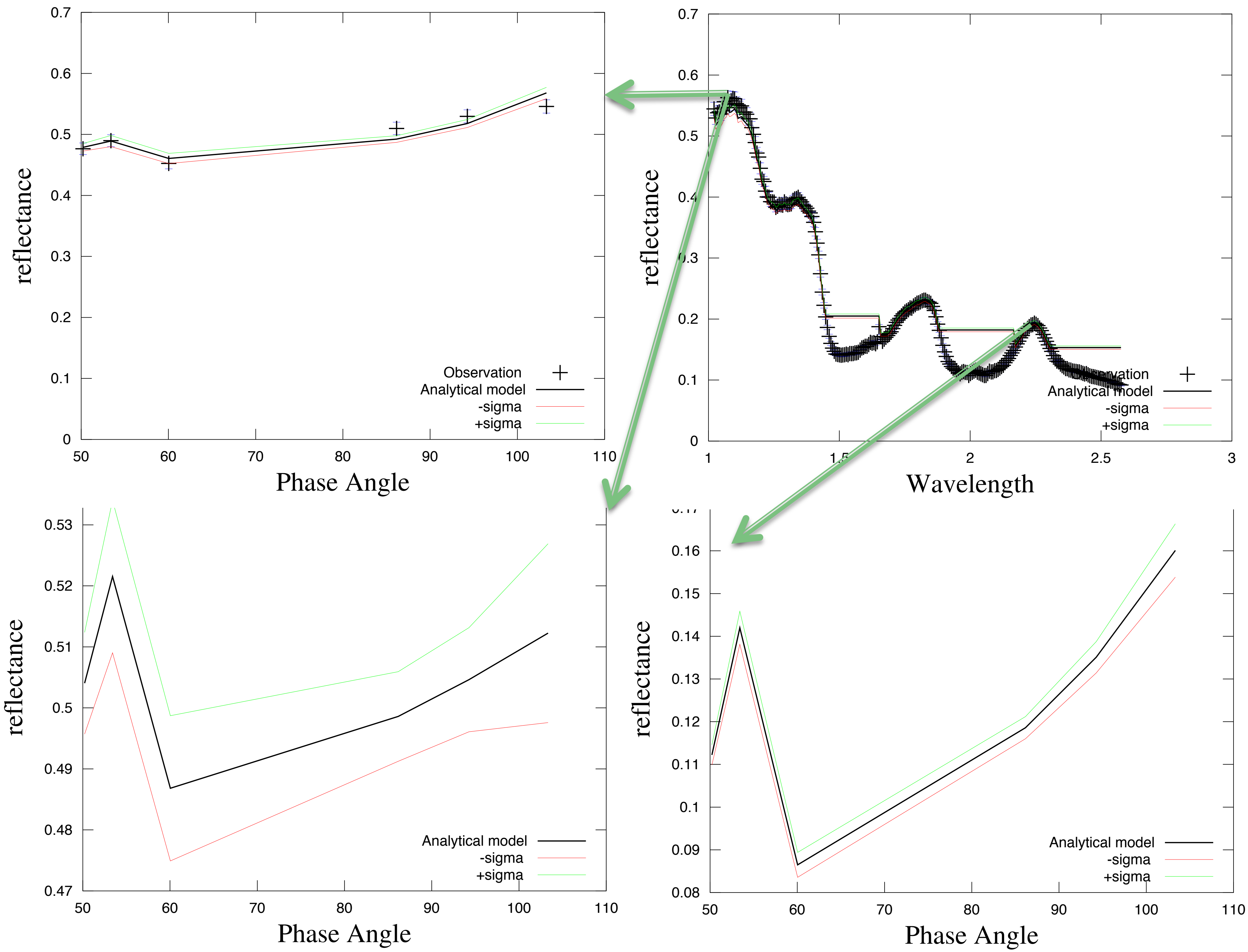

reflectance
Phase Angle
Wavelength
Observation
Analytical model
-sigma
+sigma
0
0.1
0.2
0.3
0.4
0.5
0.6
0.7
50
60
70
80
90
100
110
1
1.5
2
2.5
3
0.47
0.48
0.49
0.5
0.51
0.52
0.53
0.08
0.09
0.1
0.11
0.12
0.13
0.14
0.15
0.16

Correlation between kernel weights

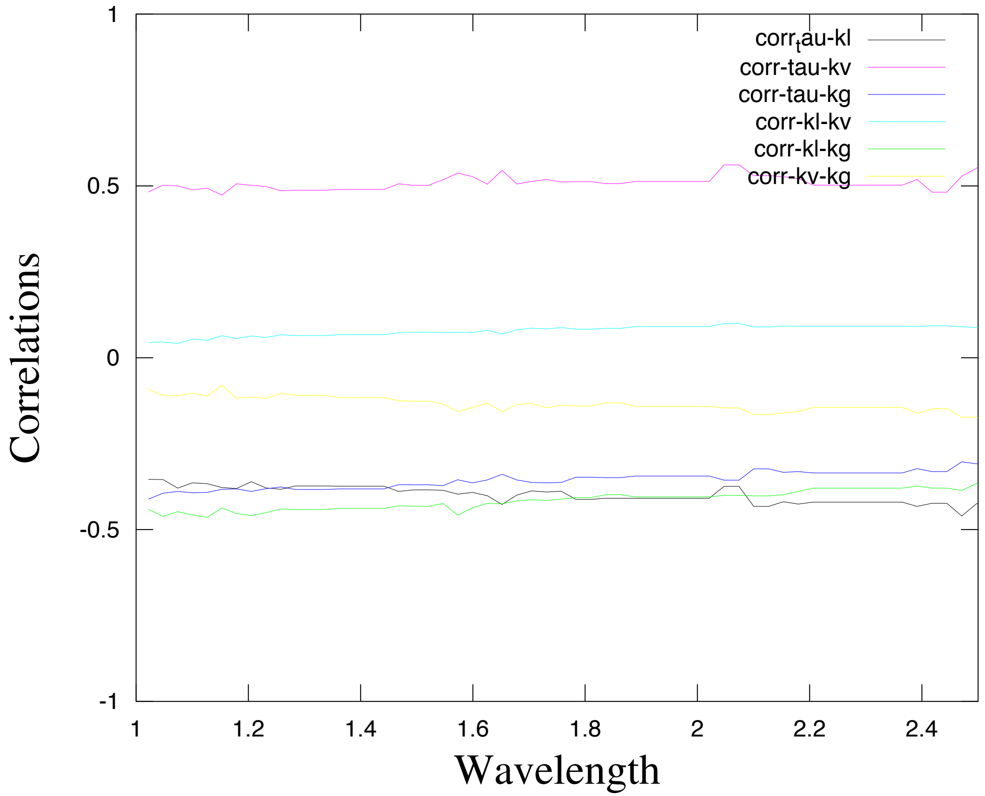

63B0

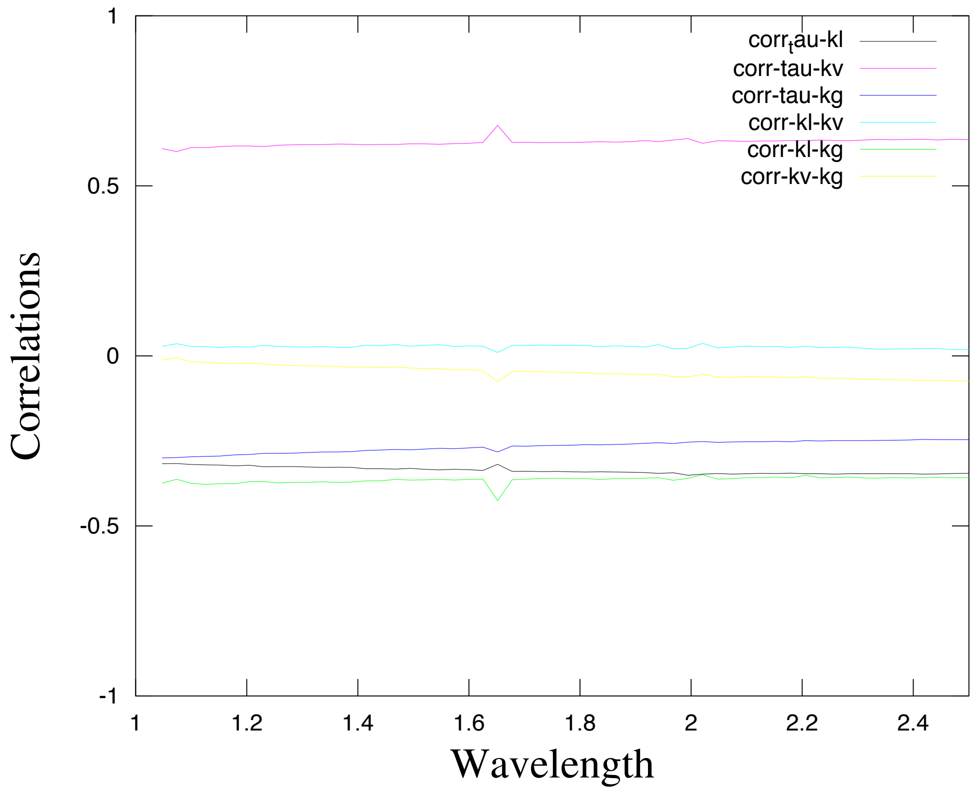

2F70

Tests on a selection of CRISM observations

CRISM ID	Site	Topo	Incidence	Phase angle range	AOT (MARS-Reco)	AOT (Wolf)	Quality index of the results (x/5)
FRT3192	Gusev	none	64.4°	56-112°	0.33	0.35	5
FRT8CE1	Gusev	none	40.2°	41-90°	0.63	0.97	1
FRTCDA5	Gusev	yes	62.8°	46-106°	0.27	0.32	3
FRT82EB	Cratered surface	yes	74.5°	31-130°		0.63	1
FRT2F70	Crater containing water ice	none	59°	49-104°	0.4	0.32	5
FRT63B0	Early Summer CO2 ice Lag	none	66.2	40-115°	0.35	1.25	5

The algorithm fails when the phase angle range is limited, the incidence angle is higher than 70°, the topography is accuentuated or perhaps a combination of these three factors